21. Okawa Y, Sugiyama K, Aiba K, Hirano A, Uno S, Hagino T, Kawase K, Shioya H, Yoshida K, Usui N, Kobayashi M and Kobayashi T: Successful combination therapy with trastuzumab and Paclitaxel for adriamycin- and docetaxel-resistant inflammatory breast cancer. Breast Cancer 11: 309-312, 2004.
22. Hayashi H, Kimura M, Yoshimoto N, Tsuzuki M, Tsunoda N, Fujita T, Yamashita T and Iwata H: A case of HER2-positive male breast cancer with lung metastases showing a good response to trastuzumab and paclitaxel treatment. Breast Cancer 16: 136-140, 2009.
23. Bullock K and Blackwell K: Clinical efficacy of taxane-trastuzumab combination regimens for HER-2-positive metastatic breast cancer. Oncologist 13: 515-525, 2008.
24. Hattori Y, Ding WX and Maitani Y: Highly efficient cationic hydroxyethylated cholesterol-based nanoparticle-mediated gene transfer in vivo and in vitro in prostate carcinoma PC-3 cells. J Control Release 120: 122-130, 2007.
25. Hattori Y, Fukushima M and Maitani Y: Non-viral delivery of the connexin 43 gene with histone deacetylase inhibitor to human nasopharyngeal tumor cells enhances gene expression and inhibits in vivo tumor growth. Int J Oncol 30: 1427-1439, 2007.
26. Hattori Y, Yoshizawa T, Koga K and Maitani Y: NaCl induced high cationic hydroxyethylated cholesterol-based nanoparticle-mediated synthetic small interfering RNA transfer into prostate carcinoma PC-3 cells. Biol Pharm Bull 31: 2294-2301, 2008.
27. Baselga J, Norton L, Albanell J, Kim YM and Mendelsohn J: Recombinant humanized anti-HER2 antibody (Herceptin) enhances the antitumor activity of paclitaxel and doxorubicin against HER2/neu overexpressing human breast cancer xenografts. Cancer Res 58: 2825-2831, 1998.
28. Fujimoto-Ouchi K, Sekiguchi F, Yasuno H, Moriya Y, Mori K and Tanaka Y: Antitumor activity of trastuzumab in combination with chemotherapy in human gastric cancer xenograft models. Cancer Chemother Pharmacol 59: 795-805, 2007.
29. Hall PS and Cameron DA: Current perspective-trastuzumab. Eur J Cancer 45: 12-18, 2009.
30. Burris H III, Yardley D, Jones S, Houston G, Broome C, Thompson D, Greco FA, White M and Hainsworth J: Phase II trial of trastuzumab followed by weekly paclitaxel/carboplatin as first-line treatment for patients with metastatic breast cancer. J Clin Oncol 22: 1621-1629, 2004.
31. Vogel CL, Cobleigh MA, Tripathy D, Gutheil JC, Harris LN, Fehrenbacher L, Slamon DJ, Murphy M, Novotny WF, Burchmore M, Shak S, Stewart SJ and Press M: Efficacy and safety of trastuzumab as a single agent in first-line treatment of HER2-overexpressing metastatic breast cancer. J Clin Oncol 20: 719-726, 2002.
32. Morris MJ, Reuter VE, Kelly WK, Slovin SF, Kenneson K, Verbel D, Osman I and Scher HI: HER-2 profiling and targeting in prostate carcinoma. Cancer 94: 980-986, 2002.
33. Lara PN Jr, Chee KG, Longmate J, Ruel C, Meyers FJ, Gray CR, Edwards RG, Gumerlock PH, Twardowski P, Doroshow JH and Gandara DR: Trastuzumab plus docetaxel in HER-2/neu-positive prostate carcinoma: final results from the California Cancer Consortium Screening and Phase II Trial. Cancer 100: 2125-2131, 2004.
34. Tanner M, Kapanen AI, Junttila T, Raheem O, Grenman S, Elo J, Elenius K and Isola J: Characterization of a novel cell line established from a patient with Herceptin-resistant breast cancer. Mol Cancer Ther 3: 1585-1592, 2004.
35. Hasegawa S, Hirashima N and Nakanishi M: Microtubule involvement in the intracellular dynamics for gene transfection mediated by cationic liposomes. Gene Ther 8: 1669-1673, 2001.
36. Nair RR, Rodgers JR and Schwarz LA: Enhancement of transgene expression by combining glucocorticoids and anti-mitotic agents during transient transfection using DNA-cationic liposomes. Mol Ther 5: 455-462, 2002.

Cancer Science
The official journal of the Japanese Cancer Association JCA

Combination of RET siRNA and irinotecan inhibited the growth of medullary thyroid carcinoma TT cells and xenografts *via* apoptosis

Kimiko Koga,[1] Yoshiyuki Hattori,[1,3] Mihoko Komori,[1] Ryota Narishima,[2] Masahiro Yamasaki,[2] Motoki Hakoshima,[1] Tetsuya Fukui[2] and Yoshie Maitani[1]

[1]Institute of Medicinal Chemistry, [2]Department of Health Chemistry, Hoshi University, Shinagawa-ku, Tokyo, Japan

(Received October 26, 2009/Revised December 16, 2009/Accepted December 19, 2009/Online publication February 5, 2010)

Medullary thyroid carcinoma (MTC) is a rare endocrine tumor that frequently metastasizes, and treatment with irinotecan (CPT-11) is limited because of side effects. Mutations in the Rearranged during transfection (RET) proto-oncogene are considered the causative event of MTC. The objective of this study was to examine whether small interfering RNA (siRNA) and its combined treatment with CPT-11 could inhibit MTC cell growth *in vitro* and *in vivo*. The transfection of RET siRNA suppressed RET expression, reduced proliferation, and increased caspase-3/7 activity *via* the down-regulation of Bcl-2 expression. Combined treatments with CPT-11 or SN-38 significantly increased caspase 3/7 activity compared with RET siRNA, CPT-11 or SN-38 treatment alone. Importantly, intratumoral injection of RET siRNA along with intravenous injection of CPT-11 significantly inhibited the tumor growth of MTC xenografts *via* an increased apoptotic effect. These findings that RET siRNA enhanced sensitivity for CPT-11 will provide a novel strategy for the treatment of MTC with RET mutation. (*Cancer Sci* 2010; 101: 941–947)

Medullary thyroid carcinoma (MTC) is a rare endocrine tumor originating from calcitonin-secreting C cells. MTC may be sporadic or hereditary, including multiple endocrine neoplasia (MEN) type 2A, MEN type 2B and familial medullary thyroid carcinoma (FMTC).[1] MTC has an overall 10-year cause-specific survival of 60–70%, with a particularly poor prognosis for patients with MEN2B and sporadic MTC, who have a 5-year mortality of 30–50%.[2] Hereditary MTC is caused by a germline mutation in the Rearranged during transfection (RET) gene. About 40% of sporadic MTCs harbor a somatic RET mutation.[1] The RET gene encodes a receptor tyrosine kinase with an extracellular ligand-binding domain and a cysteine-rich domain, a signal transmembrane domain and an intracellular domain containing the catalytic tyrosine kinase domain.[3] RET has a glial cell line-derived neurotrophic factor as a ligand,[4] but mutated RET leads to a constitutive active RET tyrosine kinase, causing malignant behavior of C cells.[5]

Surgery is currently the only effective treatment for primary MTC.[6] Radioactive iodine has no benefit since C cells do not take up iodine. The role of chemotherapeutic regimens is also limited.[7] Imatinib specifically inhibits the tyrosine kinase activity of Abl, Kit and platelet-derived growth factor receptor (PDGFR).[8] However, imatinib therapy for MTC yielded no objective responses and induced considerable toxicity in patients.[9] CPT-11 injected intraperioneally was relatively effective for TT tumor xenografts.[10] There is, therefore, no curative therapy for patients with metastatic MTC, which is responsible for many of the deaths caused by MTC. Gene therapy is a potentially useful alternative treatment for MTC. Specific inhibition of RET signaling using the dominant-negative RET mutant and ribozyme resulted in both growth suppression and subsequently the death of MTC cells.[11–13] Expressions of thymidine kinase, interleukin (IL-2) and IL-12 by adenoviral vectors have resulted in tumor suppression in MTC animal models;[14] however, the observed antitumor effect *in vivo* was mostly transient.

New technology based on specific inhibition of the RET gene may be useful for MTC treatment to improve safety. RNA interference (RNAi) is a powerful gene-silencing process that holds great promise in the field of cancer therapy.[15] Small interfering RNAs (siRNAs) are expected to have a medicinal application in human gene therapy as drugs with high specificity for molecular targeting. RET siRNA can inhibit the expression of RET tyrosine kinase receptor, and it is expected to inhibit all signals following RET tyrosine kinase; however, gene therapy with RET siRNA has not been reported *in vivo* for thyroid cells endogenously expressing mutated RET.

It is rational to select tyrosine kinase inhibitors for the treatment of MTC, although a selective drug that targets RET has not yet been found. Therefore, in this study, we selected RET siRNA as potentially therapeutic molecules. Human MTC (TT) cells endogenously expressed RET bearing the C634W mutation associated with MEN2A mutations, which have been identified mainly in one of six cysteine residues (codon 609, 611, 618, 620 in exon 10, and codon 630, 634 in exon 11) in the RET extracellular domain;[1,16] therefore, TT cells are useful as a model for studying MTC.[16]

In this study, we investigated whether the transfection of RET siRNA alone and in combination with CPT-11 could induce the growth inhibition of TT cells and tumor xenografts. Combination therapy with RET siRNA and CPT-11 may be effective for MTC.

Materials and Methods

Cell culture. TT cells were obtained from the European Collection of Cell Cultures (ECACC, Wiltshire, UK). The cells were grown in Ham's F-12 culture medium (Wako, Osaka, Japan) supplemented with 10% heat-inactivated fetal bovine serum (FBS) (Gibco BRL) at 37°C in a 5% CO_2 humidified atmosphere.

siRNA. The stealth RNA interference duplex-targeting nucleotides of RET (RET-1 siRNA, RET 2-siRNA and RET-3 siRNA) and stealth RNAi Negative Control Low GC Duplex and Medium GC Duplex as control siRNAs (Cont-L siRNA and Cont-M siRNA, respectively) were synthesized by Invitrogen (Carlsbad, CA, USA). The stealth siRNA sequences of RET were RET-1 sense: 5′-AAAUCCGAAAUCUUCAUCUUCCGCC-3′ and antisense strand 5′-GGCGGAAGAUGAAGAUUUCGGAUUU-3′, RET-2: sense 5′-AAUCCUCUUCAUAAACAUCUCGGGA-3′ and antisense 5′-UCCCGAGAUGUUUAU-

[3]To whom correspondence should be addressed. E-mail: yhattori@hoshi.ac.jp

doi: 10.1111/j.1349-7006.2009.01484.x

GAAGAGGAUU-3′, RET-3: sense 5′-AAAUCAGGGAGUCA-GAUGGAGUGGA-3′ and antisense 5′-UCCACUCCAUC-UGACUCCCUGAUUU-3′. RET siRNA cocktail is used as a cocktail of three duplexes (100 nmol of RET stealth siRNA cocktail containing 33.3 nmol of each individual siRNA).

Western blotting. TT cells were transfected at a concentration of 100 nM siRNA by Lipofectamine 2000 (Invitrogen Corp.), and then incubated for 72 h. Cell protein extracts were prepared with sampling buffer containing 1% Triton X-100 in phosphate-buffered saline pH 7.4 (PBS), and then Western blotting was performed as previously reported.[17] Expression of RET protein was identified using rabbit anti-RET polyclonal antibody (Santa Cruz Biotechnology, Inc., Santa Cruz, CA, USA) and goat anti-rabbit IgG peroxidase conjugate (Santa Cruz Biotechnology) as the secondary antibody. Expression of Bcl-2 and β-actin protein was identified as previously described.[17]

Antiproliferative activity. TT cells at 50% confluence in 96-well plates were transfected with 100 nM siRNA by Lipofectamine 2000, and then incubated for 72 h. In combination with CPT-11 or SN-38, the culture medium was exchanged for medium containing CPT-11 (Irinotecan; Yakuruto, Tokyo, Japan) ranging from 0.1 to 1000 μg/mL or SN-38 (ethyl-10-hydroxy-camptothecin; Wako, Osaka, Japan) ranging from 0.001 to 10 μg/mL 48 h after transfection of siRNA, and then incubated for another 48 h. After incubation, cell viability was measured by a cell proliferation assay kit (Dojindo, Kumamoto, Japan) as previously reported.[17]

The numbers of dead cells after treatment with RET siRNA, CPT-11, SN-38 or their combination were measured by propidium iodide (PI) staining. The cells were transfected with 100 nM siRNA and then incubated for 48 h. The culture medium was exchanged for medium containing 10 μg/mL CPT-11 or 0.2 μg/mL SN-38, and then incubated for another 48 h. The percentage of PI-positive cells was determined by examining fluorescence intensity on a FACSCalibur flow cytometer (Becton Dickinson, San Jose, CA, USA) as previously described.[17]

Real-time RT-PCR for quantification of RET and Bcl-2 mRNA. TT cells at 50% confluence in 6-well plates were transfected with 100 nM siRNA with Lipofectamine 2000 and then incubated for 72 h. Total RNA was isolated from transfected cells using the NucleoSpin RNA II (Macherey-Nagel, Dueren, Germany). SYBR green quantitative RT-PCR amplification for Bcl-2 and β-actin cDNA was carried out by MyiQ™ Single Color Real-Time PCR Detection System (Bio-Rad Laboratories, Hercules, CA, USA) as previously reported.[17] For the amplification of human RET cDNA, primers RET-FW, 5′-GGCAGC-CAGAAACATCCT-3′, and RET-RW, 5′-ACTTTGCGTGGTG-TAGAT-3′, were used.

Caspase 3/7 assay. TT cells at 50% confluence in 12-well plates were transfected with 100 nM siRNA using Lipofectamine 2000 and then incubated for 48 h. The culture medium was then exchanged for medium containing 10 μg/mL CPT-11 or 0.2 μg/mL SN-38 and then incubated for another 48 h. After the incubation, caspase 3/7 activity was measured by Caspase3/7 assay system (Caspase-Glo® 3/7 assay; Promega, Madison, WI, USA) as previously reported.[18]

Assessment of TT tumor growth. Female ICR nu/nu mice (6 weeks of age) were purchased from Oriental Yeast Co., Ltd. (Tokyo, Japan). To generate TT tumor xenografts, 1×10^7 TT cells suspended in 50 μL PBS containing 50% Matrigel (Collaborative Research, Bedford, MA, USA) were inoculated subcutaneously into the flank region of mice. When the average volume of xenograft tumors reached about 100 mm^3, therapy was started (day 0). For siRNA transfection *in vivo*, we used cationic nanoparticles (NP) consisting of cholesteryl-3β-carboxyamidoethylene-*N*-hydroxyethylamine as a cationic lipid, and 5 mol% Tween-80, as previously reported.[19] For transfection into tumors, 10 μg siRNA was mixed with NP at a charge ratio (+/−) of cationic lipid/siRNA of 1/1 with gentle shaking and standing for 15 min at room temperature. The complex of NP and siRNA was directly injected into the xenografts on days 0, 3, and 6, and CPT-11 was intravenously injected at a dose of 30 mg/kg on day 2, 5, and 8. On 24 days, blood was collected into tubes and centrifuged to separate plasma from blood cells. Serum concentrations of calcitonin were measured using a human calcitonin ELISA kit (Biosource International, Inc., CA, USA). Animal experiments were conducted with ethics approval from our institutional animal care and use committee.

Preparation of probes for *in situ* hybridization. The RET cDNA fragment (873 bp) was amplified from TT cells cDNA. The RET primers used for RET cDNA amplification were: forward primer, 5′-TCCTGGGAGAAGCTCAGTGT-3′ and reverse primer, 5′-CACGTTGAAGTGGAGCAAGA-3′. The fragments were cloned into pGEM-T vector (Promega), and ^{35}S-labeled cRNA probes were prepared as previously reported.[20]

***In situ* hybridization.** For transfection into tumors, the complex of NP and 10 μg siRNA per tumor was directly injected into TT tumor xenografts on days 0, 3, and 6. At 48 h after final injection the tumors were frozen in powdered dry ice, and

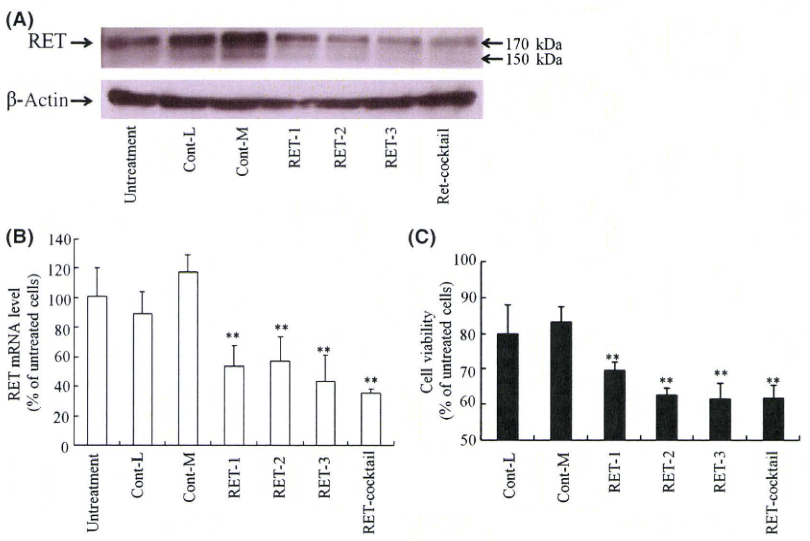

Fig. 1. Inhibition of RET expression by transfection of RET siRNA with Lipofectamine 2000 into TT cells. Expressions of RET protein (170 KDa) and mRNA were detected by Western blot (A) and quantitative RT-PCR (B) analyses, respectively, 72 h after transfection with 100 nM Cont-L and -M siRNA, RET-1, -2 and -3 siRNA and their cocktail. The number of viable cells was determined by WST-8 assay 72 h after transfection (C). $n = 4$ for each sample. $^{**}P < 0.01$, compared with Cont-L siRNA transfected cells.

doi: 10.1111/j.1349-7006.2009.01484.x

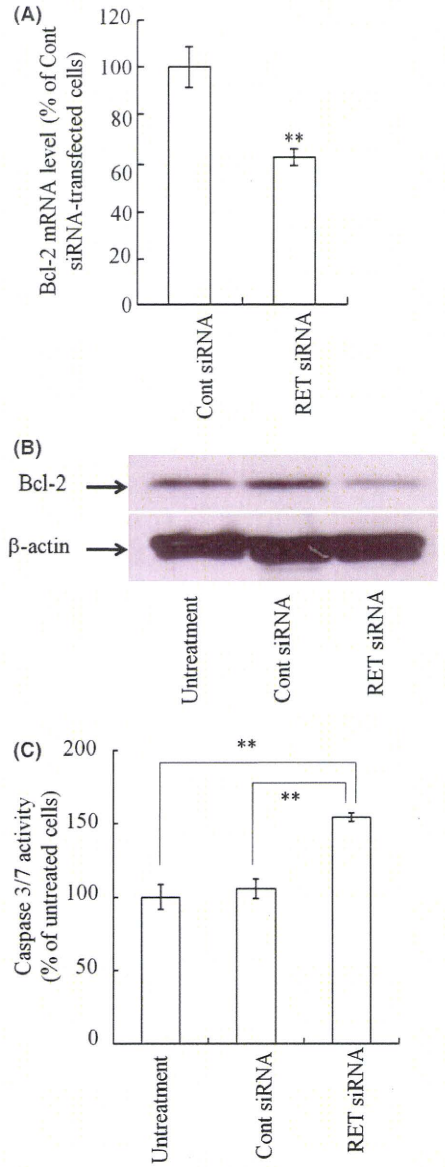

Fig. 2. Effect of transfection with RET siRNA with Lipofectamine 2000 on Bcl-2 expression and caspase 3/7 activity in TT cells. Cells were incubated for 72 h after transfection with 100 nM RET siRNA or Cont siRNA. Expressions of Bcl-2 mRNA and protein were detected by quantitative RT-PCR (A) and Western blot (B). Caspase 3/7 activity was measured by caspase 3/7 luminometric assay (C). $n = 4$ for each sample. $^{**}P < 0.01$.

coronal sections were cut 16 μm thick with a cryostat, thaw-mounted onto gelatin and poly-lysine-coated slides. *In situ* hybridization was carried out as previously described.[20] All sections were counterstained with hematoxylin and eosin.

***In vivo* detection of apoptosis.** For siRNA transfection into tumors, 10 μg siRNA per tumor was directly injected by NP into TT tumor xenografts on days 0, 3, and 6. CPT-11 was intravenously injected at a dose of 30 mg/kg on day 2, 5, and 8. On day 11, the Red *in vivo* FLIVO™ apoptosis Kit (Immunochemistry Technologies, Bloomington, MN, USA) was injected *i.v.* and allowed to circulate for 30 min. The tumors were frozen in powdered dry ice, and coronal sections were cut 20 μm thick with a cryostat, thaw-mounted onto poly-lysine-coated slides. The specimens were examined microscopically using an Eclipse TS100-F microscope (Nikon, Tokyo, Japan).

Statistical analysis. The statistical significance of the data was evaluated with Student's *t*-test. $P < 0.05$ was considered significant.

Results

***In vitro* growth inhibitory effect of RET siRNA.** We initially characterized the expression of RET protein in TT cells after transfection of RET siRNA with Lipofectamine 2000. Here, we used RET-1, RET-2, RET-3 and their cocktail siRNAs as RET siRNAs (40%, 44%, 48%, and 44% in GC contents of the siRNA sequence, respectively), and Cont-L and -M siRNAs as negative control siRNAs (36% and 48% in GC contents of the siRNA sequence, respectively). Expression of RET protein was strongly suppressed in TT cells 48 h after transfection of RET-1, RET-2, RET-3 siRNA or their siRNA cocktail, but unaffected by the transfection of Cont-L or -M siRNA (Fig. 1A). Furthermore, the transfection of RET siRNA suppressed the expression of RET mRNA to about 40–50% of untransfected cells (Fig. 1B).

To investigate whether the suppression of RET expression induced the inhibition of cell growth, we examined cell viability 72 h after transfection of RET siRNA at 100 nM. After transfection, the cell viabilities of all RET siRNAs were 60–70%, but those of Cont-L and -M were 80 and 83%, respectively (Fig. 1C). When transfected at a concentration of 12.5 nM siRNA, the RET siRNA cocktail showed a stronger decrease of cell viability (67%) than RET-1, RET-2 and RET-3 siRNA (76, 72, and 75%, respectively) (data not shown). The slight inhibition of cell growth by transfection with Cont-L and -M siRNA may be due to the toxicity of Lipofectamine 2000. In subsequent studies, we used the RET siRNA cocktail as a RET siRNA, and Cont-L siRNA as a control siRNA.

Bcl-2 expression and caspase 3/7 activity after transfection with RET siRNA into TT cells. It has been reported that the expression of a dominant-negative RET down-regulated the expression of Bcl-2.[21] Therefore, we investigated whether transfection of RET siRNA affected Bcl-2 expression in TT cells (Fig. 2A,B). Transfection of RET siRNA decreased the expression of Bcl-2 mRNA and protein (Fig. 2A,B) and furthermore, significantly increased caspase 3/7 activity in cells compared with Cont siRNA (Fig. 2C). These findings suggested that the suppression of RET expression may increase caspase 3/7 activity *via* the down-regulation of Bcl-2 expression.

***In vitro* sensitivity of CPT-11 or SN-38.** Here, we used CPT-11 as a potent antitumor drug for TT tumor xenografts, because it has been reported that MTC cell lines were sensitive to a topoisomerase I inhibitor, camptothecin (CPT).[22] To investigate whether the transfection of RET siRNA enhanced sensitivity for chemotherapy, we incubated CPT-11 or its active metabolite SN-38 for 48 h in the cells 48 h after transfection of RET siRNA. In cells transfected with RET siRNA, cytotoxicities by CPT-11 and SN-38 were similar with those in cells transfected with Cont siRNA (Fig. 3A,B), indicating that their activities were at least additive for tumor suppression by RET siRNA.

We next investigated whether RET siRNA transfection affected the number of cell deaths and caspase 3/7 activity by CPT-11 or SN-38 treatment. The cells were transfected with RET or Cont siRNA for 48 h, and then treated with 10 μg/mL CPT-11 or 0.2 μg/mL SN-38 for 48 h, the concentrations of which were around the IC_{50} of CPT-11 and SN-38 in untransfected cells, respectively. To measure the number of cell deaths, PI staining of the cellular nucleus was used as a marker. RET siRNA transfection increased the number of PI-staining cells and caspase 3/7 activity compared with Cont siRNA

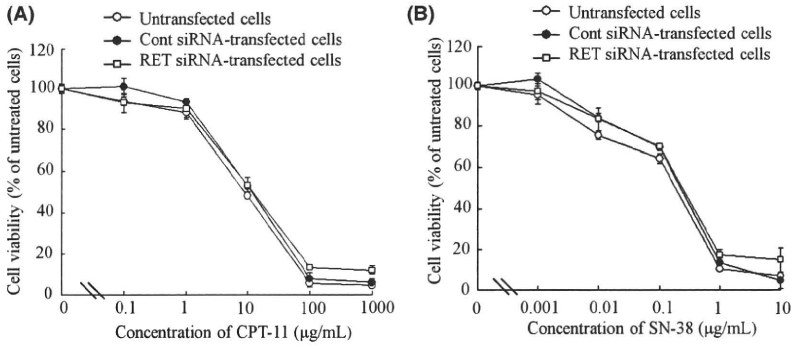

Fig. 3. Concentration-dependent effect of CPT-11 or SN-38 on cytotoxicity after transfection with RET siRNA. Cells were transfected with 100 nM RET siRNA or Cont siRNA with Lipofectamine 2000 and incubated for 48 h. After incubation, the cells were treated with various concentrations of CPT-11 (A) or SN-38 (B) and incubated for another 48 h. The number of viable cells was determined by WST-8 assay. $n = 4$ for each sample.

transfection (Fig. 4A,B). Among treatments, the combination of RET siRNA plus SN-38 significantly increased activity and cells compared to RET siRNA or SN-38 alone (Fig. 4A,B) ($P < 0.01$).

Suppression of RET expression in TT tumor xenografts. Next, we investigated whether the expression of RET mRNA was decreased by intratumoral injection of RET siRNA. Here, we used NP as a siRNA transfection vector for *in vivo* experiments.[19] Cont or RET siRNA was directly injected with NP into TT tumor xenografs 3 times at 3-day intervals and then tumors were excised 2 days after the final injection. The sense probe for the RET gene was used as a negative control probe. Silver grain distribution in the dark field and black grain in the bright field following *in situ* hybridization exhibiting RET mRNA expression (Fig. 5A,B, supplemental Figs S1 and S2). Positive cells for RET mRNA were strongly detected in the tumor cells, but not stroma cells with the antisense probe for the RET gene (Fig. 5B). Most of the tumor cells were positive for the expression of RET mRNA in saline-injected and Cont siRNA-transfected cells. In contrast, RET siRNA transfection decreased the number of silver grains in the dark field (Fig. 5A) and black grains in the bright field (Fig. 5B) in some tumor sections, indicated that the expression of RET mRNA was suppressed by RET siRNA injection.

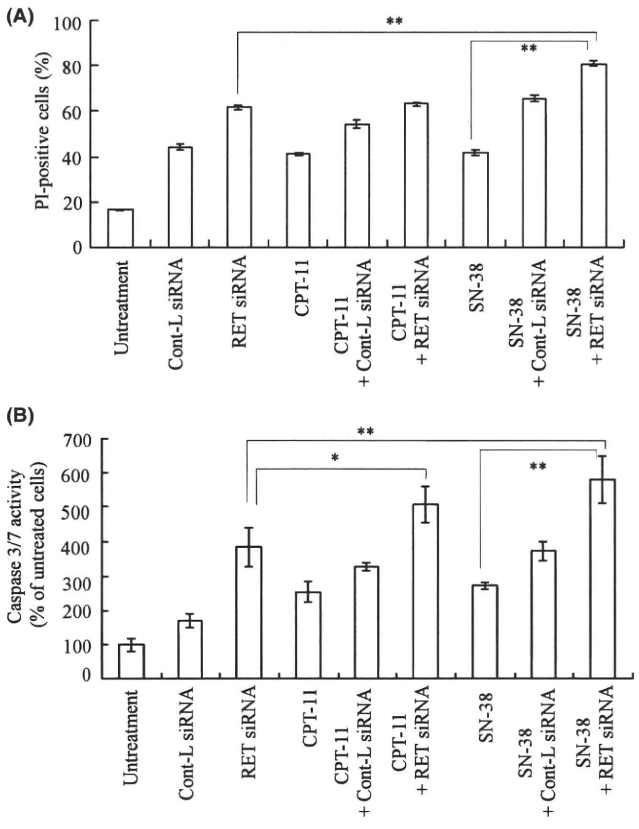

Fig. 4. Dead cells (A) and caspase-3/7 activity (B) by combined treatment with RET siRNA plus CPT-11 or SN-38 in TT cells. The number of dead cells was measured by a FACSCalibur flow cytometer after staining with PI (A). Caspase-3/7 activity was measured by caspase-3/7 luminometric assay (B). $n = 3$ for each sample. $*P < 0.05$, $**P < 0.01$; compared with RET siRNA transfected cells.

Synergistic inhibition of the growth of TT tumor xenografts. We evaluated the efficacy of combination therapy of RET siRNA and CPT-11 in inhibiting the growth of subcutaneous TT tumors. The anti-tumor effect was evaluated by direct injection of Cont or RET siRNA with NP into xenografts once a day three times (day 0, 3, and 6) following three *i.v.* injections of CPT-11 (day 2, 5, and 8). No significant growth inhibitory effect was observed in mice treated with RET siRNA, CPT-11 or CPT-11 plus Cont siRNA compared with mice injected with saline (Fig. 6A). CPT-11 plus Cont siRNA exhibited a similar tumor suppressive effect with CPT-11 alone. A significant growth inhibitory effect was observed in combination therapy with CPT-11 and RET siRNA compared with CPT-11 alone. All treatments, the transfection of RET siRNA, the injection of CPT-11 alone, and their combination did not significantly change body weight during 3 weeks of treatment (data not shown). In this study, the effect of the combination on tumor growth was significantly higher than that of CPT-11 alone at lower doses that did not exhibit serve adverse effects.

RET siRNA transfection alone could not significantly suppress tumor growth. The results of *in situ* hybridization showed that the suppression of RET expression in the tumors was restricted to the tumor in the vicinity of the injection site (data not shown). Strong inhibition of *in vivo* tumor growth by RET siRNA depends on the development of a gene vector having the ability to introduce siRNA widely into tumors.

Serum calcitonin concentration and *in vivo* apoptosis. C cells of the thyroid gland secrete calcitonin, the level of which is elevated in patients with C cell hyperplasia and MTC; therefore, calcitonin is a very sensitive and reliable marker for the presence of MTC, and the level of calcitonin correlates with tumor burden and the response to therapy.[23,24] On day 24 in Fig. 6A, all mice were sacrificed, and serum calcitonin concentration was measured. Serum calcitonin level in TT tumor xenografts showed a 21-fold increase compared with that in normal mice (Fig. 6B). RET siRNA or CPT-11 alone decreased serum calcitonin levels to 39% and 80% compared with saline (Fig. 6B). Corresponding to the highest growth inhibition, the combination of CPT-11 plus RET siRNA markedly decreased the serum calcitonin level to 30%.

To confirm the effectiveness *in vivo*, we detected apoptotic cells 48 h after combination therapy with RET siRNA and

doi: 10.1111/j.1349-7006.2009.01484.x

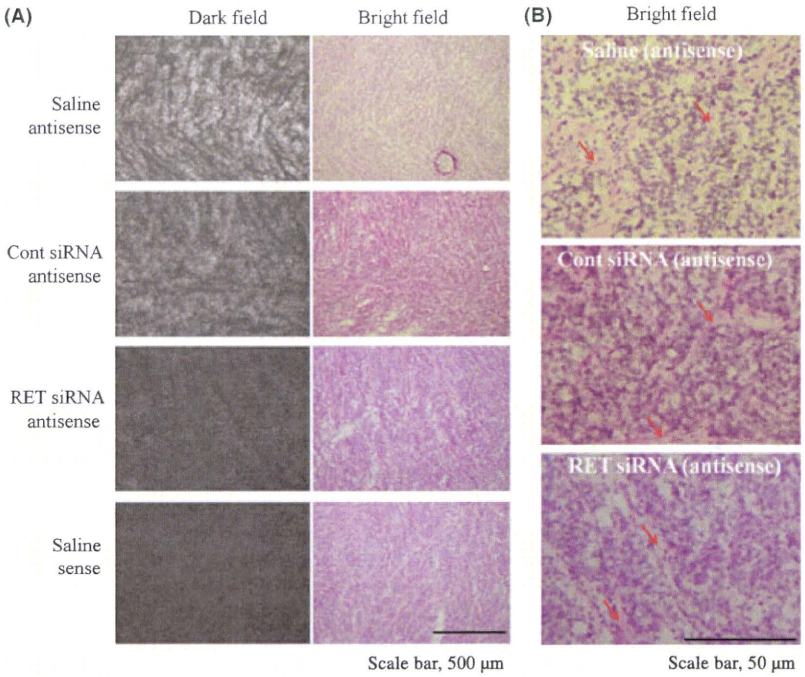

Fig. 5. *In situ* hybridization of a ^{35}S-labeled antisense or sense probe generated against RET mRNA. An antisense probe was used to detect RET mRNA. The sense probe for the RET gene was used as a negative control probe. In (A), silver grains in a dark field indicate RET mRNA expression. Scale bar: 500 μm. In (B), microautoradiographs in bright fields in Fig. 5(A) were enlarged. Black grains indicate RET mRNA expression. Red arrows indicate stroma cells. Scale bar: 50 μm.

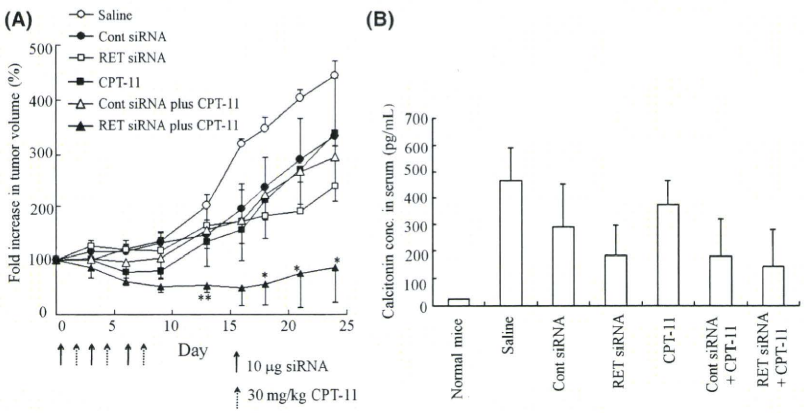

Fig. 6. *In vivo* combination therapy of RET siRNA and CPT-11 for TT tumor xenografts. Ten microgram of RET or Cont siRNA per tumor was directly injected with NP into the tumor on days 0, 3, and 6. CPT-11 at a dose of 30 mg/kg was injected *i.v.* on days 2, 5, and 8. Tumor volume was measured for 24 days (A). $*P < 0.05$, $**P < 0.01$; compared with the group injected with CPT-11. All mice were sacrificed on day 24 and the concentration of calcitonin in blood was measured (B). Data in A and B are shown as the mean ± SE. $n = 3$ for each group.

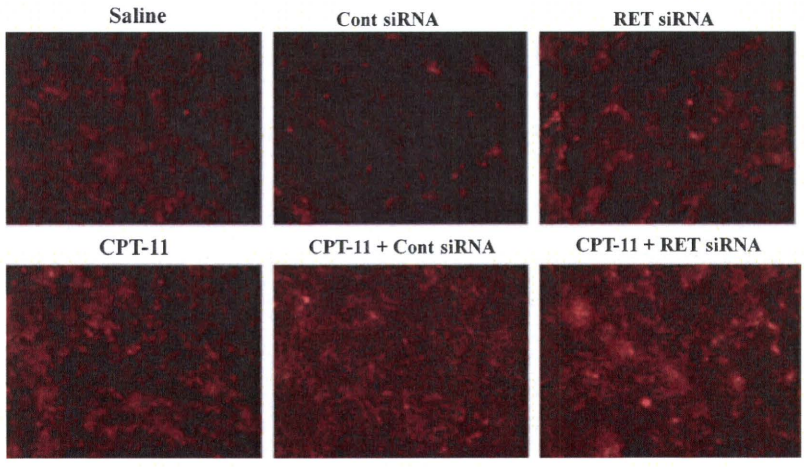

Fig. 7. Distribution of apoptotic cells in TT tumor xenografts after injection of RET siRNA and CPT-11. Experimental conditions were the same as in Fig 6. On day 11, all mice were sacrificed and apoptosis cells were detected by the Red *in vivo* FLIVO™ apoptosis Kit. Red signals indicate apoptotic cells. Magnification ×100.

CPT-11. In tumor sections after injections of RET siRNA or CPT-11 alone, red, indicating apoptotic cells, was slightly observed, but not in saline or Cont siRNA (Fig. 7). On the other hand, combination treatment with RET siRNA plus CPT-11 strongly induced apoptotic cells. These data also indicated that combination therapy was effective for MTC.

Discussion

In this study, we demonstrated that the combination with RET siRNA and CPT-11 could induce the growth inhibition of TT cells and tumor xenografts. Recently, RET siRNA delivered by chitosan-coated poly(isobutylcyanoacrylate) nanoparticles led to tumor growth inhibition after intratumoral administration in mice transplanted with NIH3T3 cells transformed with the ret/PTC1 gene;[25] however, it has been reported that the ret/PTC-1 signaling pathway was different between thyroid and fibroblast cells;[26] therefore, this is the first report that RET siRNA transfected with NP inhibited tumor growth in mice bearing TT cells.

The combination therapy *in vivo* revealed greater than additive effects in cytotoxicity *in vitro*. CPT-11 is known as an effective inhibitor of angiogenesis for endothelial cells in tumor as well as cytotoxic drug.[27] The mechanism of increasing growth inhibition for TT tumor xenografts by RET siRNA and CPT-11 was not clear, although inhibition of receptor tyrosine kinase in tumor cells could sensitize cells to CPT-11.[28,29] Overexpression of Bcl-2 has been observed in MTC,[30,31] and is associated with the poor response of MTC to chemotherapy. The expression of dominant-negative RET in TT cells decreased the expression of Bcl-2 and could reduce cell viability,[21] and the antitumor effect by CPT-11 was enhanced by the combination with RET inhibitor, CEP-751, for TT tumor xenografts.[10] As another possibility, RET has been shown to activate nuclear factor κB (NFκB) *via* the phosphatidylinositol-3-kinase/Akt pathway.[1] Akt mediates multiple cellular responses, such as survival signaling by NFκB activation and BAD inactivation, and cell cycle progression; therefore, inhibition of RET expression might modulate cellular sensitivity through the survival signaling pathway.[32,33] From these findings, the combination of RET siRNA and CPT-11 will have great potential for gene therapy in MTC.

In conclusion, we demonstrated that combining RET siRNA with CPT-11 resulted in significant greater growth suppression of TT cells and tumor xenografts *via* increased apoptosis. As the thyroid gland is anatomically accessible, future treatment of primary MTC tumors by direct intratumoral injection of siRNA/NP complex expressing mutated genes is possible. Thus, the combination of RET siRNA and CPT-11 may serve as a novel tool for gene therapy.

Acknowledgments

We thank Ms. Manami Kubo for assistance with the experimental work. This study was supported in part by the Japan Health Sciences Foundation, by the Ministry of Education, Culture, Sports, Science and Technology of Japan, and by the Open Research Center Project.

References

1 Kodama Y, Asai N, Kawai K *et al.* The RET proto-oncogene: a molecular therapeutic target in thyroid cancer. *Cancer Sci* 2005; **96**: 143–8.
2 Moley JF. Medullary thyroid carcinoma. *Curr Treat Options Oncol* 2003; **4**: 339–47.
3 Hansford JR, Mulligan LM. Multiple endocrine neoplasia type 2 and RET: from neoplasia to neurogenesis. *J Med Genet* 2000; **37**: 817–27.
4 Treanor JJ, Goodman L, de SF *et al.* Characterization of a multicomponent receptor for GDNF. *Nature* 1996; **382**: 80–3.
5 Santoro M, Melillo RM, Carlomagno F, Vecchio G, Fusco A. Minireview: RET: normal and abnormal functions. *Endocrinology* 2004; **145**: 5448–51.
6 Cohen MS, Moley JF. Surgical treatment of medullary thyroid carcinoma. *J Intern Med* 2003; **253**: 616–26.
7 Gimm O. Thyroid cancer. *Cancer Lett* 2001; **163**: 143–56.
8 Jones RL, Judson IR. The development and application of imatinib. *Expert Opin Drug Saf* 2005; **4**: 183–91.
9 de Groot JW, Zonnenberg BA, van Ufford-Mannesse PQ *et al.* A phase II trial of imatinib therapy for metastatic medullary thyroid carcinoma. *J Clin Endocrinol Metab* 2007; **92**: 3466–9.
10 Strock CJ, Park JI, Rosen DM *et al.* Activity of irinotecan and the tyrosine kinase inhibitor CEP-751 in medullary thyroid cancer. *J Clin Endocrinol Metab* 2006; **91**: 79–84.
11 Drosten M, Frilling A, Stiewe T, Putzer BM. A new therapeutic approach in medullary thyroid cancer treatment: inhibition of oncogenic RET signaling by adenoviral vector-mediated expression of a dominant-negative RET mutant. *Surgery* 2002; **132**: 991–7.
12 Drosten M, Stiewe T, Putzer BM. Antitumor capacity of a dominant-negative RET proto-oncogene mutant in a medullary thyroid carcinoma model. *Hum Gene Ther* 2003; **14**: 971–82.
13 Parthasarathy R, Cote GJ, Gagel RF. Hammerhead ribozyme-mediated inactivation of mutant RET in medullary thyroid carcinoma. *Cancer Res* 1999; **59**: 3911–4.
14 Messina M, Robinson BG. Technology insight: gene therapy and its potential role in the treatment of medullary thyroid carcinoma. *Nat Clin Pract Endocrinol Metab* 2007; **3**: 290–301.
15 Pai SI, Lin YY, Macaes B, Meneshian A, Hung CF, Wu TC. Prospects of RNA interference therapy for cancer. *Gene Ther* 2006; **13**: 464–77.
16 Marsh DJ, Theodosopoulos G, Martin-Schulte K *et al.* Genome-wide copy number imbalances identified in familial and sporadic medullary thyroid carcinoma. *J Clin Endocrinol Metab* 2003; **88**: 1866–72.
17 Hattori Y, Yoshizawa T, Koga K, Maitani Y. NaCl induced high cationic hydroxyethylated cholesterol-based nanoparticle-mediated synthetic small interfering RNA transfer into prostate carcinoma PC-3 cells. *Biol Pharm Bull* 2008; **31**: 2294–301.
18 Hattori Y, Fukushima M, Maitani Y. Non-viral delivery of the connexin 43 gene with histone deacetylase inhibitor to human nasopharyngeal tumor cells enhances gene expression and inhibits in vivo tumor growth. *Int J Oncol* 2007; **30**: 1427–39.
19 Yoshizawa T, Hattori Y, Hakoshima M, Koga K, Maitani Y. Folate-linked lipid-based nanoparticles for synthetic siRNA delivery in KB tumor xenografts. *Eur J Pharm Biopharm* 2008; **70**: 718–25.
20 Hattori Y, Koga K, Izumisawa T *et al.* The distribution of mRNA expression and protein after hydrodynamic injection of transgene in mice. *Biol Pharm Bull* 2009; **32**: 755–9.
21 Drosten M, Hilken G, Bockmann M *et al.* Role of MEN2A-derived RET in maintenance and proliferation of medullary thyroid carcinoma. *J Natl Cancer Inst* 2004; **96**: 1231–9.
22 Kaczirek K, Schindl M, Weinhausel A *et al.* Cytotoxic activity of camptothecin and paclitaxel in newly established continuous human medullary thyroid carcinoma cell lines. *J Clin Endocrinol Metab* 2004; **89**: 2397–401.
23 Moley JF, Wells SA, Dilley WG, Tisell LE. Reoperation for recurrent or persistent medullary thyroid cancer. *Surgery* 1993; **114**: 1090–5.
24 Tisell LE, Dilley WG, Wells SA Jr. Progression of postoperative residual medullary thyroid carcinoma as monitored by plasma calcitonin levels. *Surgery* 1996; **119**: 34–9.
25 de MH, Bertrand JR, Fusco A *et al.* siRNA nanoformulation against the ret/PTC1 junction oncogene is efficient in an in vivo model of papillary thyroid carcinoma. *Nucleic Acids Res* 2008; **36**: e2.
26 Barone MV, Sepe L, Melillo RM *et al.* RET/PTC1 oncogene signaling in PC Cl 3 thyroid cells requires the small GTP-binding protein Rho. *Oncogene* 2001; **20**: 6973–82.
27 Ji Y, Hayashi K, Amoh Y *et al.* The camptothecin derivative CPT-11 inhibits angiogenesis in a dual-color imageable orthotopic metastatic nude mouse model of human colon cancer. *Anticancer Res* 2007; **27**: 713–8.
28 Koizumi F, Kanzawa F, Ueda Y *et al.* Synergistic interaction between the EGFR tyrosine kinase inhibitor gefitinib ("Iressa") and the DNA topoisomerase I inhibitor CPT-11 (irinotecan) in human colorectal cancer cells. *Int J Cancer* 2004; **108**: 464–72.
29 Shao RG, Cao CX, Shimizu T, O'Connor PM, Kohn KW, Pommier Y. Abrogation of an S-phase checkpoint and potentiation of camptothecin cytotoxicity by 7-hydroxystaurosporine (UCN-01) in human cancer cell lines, possibly influenced by p53 function. *Cancer Res* 1997; **57**: 4029–35.
30 Wang HG, Reed JC. Mechanisms of Bcl-2 protein function. *Histol Histopathol* 1998; **13**: 521–30.

doi: 10.1111/j.1349-7006.2009.01484.x

31 Hinze R, Gimm O, Taubert H *et al.* Regulation of proliferation and apoptosis in sporadic and hereditary medullary thyroid carcinomas and their putative precursor lesions. *Virchows Arch* 2000; **437**: 256–63.
32 Ludwig L, Kessler H, Wagner M *et al.* Nuclear factor-kappaB is constitutively active in C-cell carcinoma and required for RET-induced transformation. *Cancer Res* 2001; **61**: 4526–35.
33 Segouffin-Cariou C, Billaud M. Transforming ability of MEN2A-RET requires activation of the phosphatidylinositol 3-kinase/AKT signaling pathway. *J Biol Chem* 2000; **275**: 3568–76.

Supporting Information

Additional Supporting Information may be found in the online version of this article:

Fig. S1. *In situ* hybridization of a ^{35}S-labeled antisense or sense probe generated against RET mRNA. Microautoradiographs in bright fields of Fig. 5A were enlarged. Black grains indicate RET mRNA expression. Scale bar: 500 μm.

Fig. S2. *In situ* hybridization of a ^{35}S-labeled antisense or sense probe generated against RET mRNA. Microautoradiographs in bright fields of Fig. 5B were enlarged. Black grains indicate RET mRNA expression. Scale bar: 50 μm.

Please note: Wiley-Blackwell are not responsible for the content or functionality of any supporting materials supplied by the authors. Any queries (other than missing material) should be directed to the corresponding author for the article.

Pharmaceutical Research, Vol. 27, No. 2, February 2010 (© 2009)
DOI: 10.1007/s11095-009-0018-9

Research Paper

Accelerated Blood Clearance Was Not Induced for a Gadolinium-Containing PEG-poly(L-lysine)-Based Polymeric Micelle in Mice

Huili Ma,[1] Kouichi Shiraishi,[2] Takuya Minowa,[1] Kumi Kawano,[1] Masayuki Yokoyama,[2,3] Yoshiyuki Hattori,[1] and Yoshie Maitani[1,4]

Received July 6, 2009; accepted November 24, 2009; published online December 25, 2009

Purpose. Accelerated blood clearance (ABC) is induced by repeated injections of PEGylated liposomes. In this study, the ABC was investigated for a gadolinium-containing PEG-poly(L-lysine)-based polymeric micelle (Gd-micelle) and PEGylated liposome (Gd-liposome) in mice.

Materials and Methods. Effects of the first injection of Gd-micelle on the tissue distribution of the second dose of Gd-micelle were studied. Additionally, effects of the first injection of Gd-micelle, Gd-liposome, empty liposome, polyethyleneglycol ($PEG_{500,000}$), and PEG-lipid on the distribution of the second dose of the Gd-liposome were evaluated.

Results. Results indicated that the tissue distribution of the second injection of the Gd-micelle at a dose of 33, 5, or 2 μmol Gd/kg was not affected by the first injection of the Gd-micelle at different doses and time intervals or of the empty PEGylated liposome 7 days before. ABC of Gd-liposome at a dose of 2.3 μmol Gd/kg (corresponding to 10 μmol lipids/kg) was observed when the empty PEGylated liposome or Gd-liposome, but not the Gd-micelle, $PEG_{500,000}$ or PEG-lipid, was pre-administered.

Conclusions. The hydrophobic core of the micelle or lipid bilayer of PEGylated liposome has a major effect on this phenomenon. These studies have significant implications for the evaluation of PEG-poly (L-lysine)-based micellar formulation of Gd-based contrast agents.

KEY WORDS: accelerated blood clearance; gadolinium; PEGylated liposome; polyethylene glycol (PEG); polymeric micelle.

INTRODUCTION

Long-circulating liposomes with surface-modified polyethyleneglycol (PEG) are often used as carriers of therapeutic agents, since they avoid capture by the reticuloendothelial system (RES) and can extend the systemic circulation time of agents, thereby improving drug delivery (1,2). It was hypothesized that PEG on the surface of liposomes forms a water shell, resulting in decreased adsorption of opsonins and subsequent phagocytosis by cells of the RES (3,4). However, PEGylated liposomes are known to lose their long-circulating property with multiple dosing. Recently, it has been reported that the first dose of PEGylated liposomes injected intravenously caused a loss of the long-circulating property and extensive accumulation in the liver at the second dose injected several days later in mice, rats, rabbit, and rhesus monkeys (5–11), a phenomenon known as accelerated blood clearance (ABC). Besides PEGylated liposomes, other nanocarriers, such as nanoparticles containing PEG, also produced this phenomenon (12). Therefore, ABC would have a significant impact on the application of long-circulating liposomes and nanoparticles with multiple administrations. In clinical applications of liposomal carriers, Gabizon *et al.* reported a reduced clearance of doxorubicin-containing PEGylated liposome in the repeated injections. This opposite behavior to the ABC phenomenon resulted from toxic activity of the encapsulated doxorubicin against the RES (13). Presently, the ABC phenomenon is not a problem in a cancer chemotherapy by the use of a PEG-liposomal carrier, whereas the ABC phenomenon in human clinics must be important for less toxic drug or gene delivery applications of the PEGylated liposomes.

To date, studies of ABC have focused mainly on PEGylated liposomes. Many factors can affect the extent to which ABC is induced by PEGylated liposomes. First of all, the dose of lipid plays an important role, with ABC enhanced at lower concentrations of lipid (6,7,12). Second, ABC occurs in a time-dependent manner (5,7). The time interval between the first and second doses is a key factor. Third, when the amount of PEGylated lipid in the first injection was ≤5 mol%, the second dose of PEGylated liposomes was eliminated more quickly from plasma than liposomes containing >10 mol% PEGylated lipid injected as a first dose (7,8). In addition, the ABC phenomenon

[1] Institute of Medicinal Chemistry, Hoshi University, 2-4-41 Ebara, Shinagawa-ku, Tokyo 142-8501, Japan.
[2] Kanagawa Academy of Science and Technology, Yokoyama "Nanomedical Polymer" Project, KSP East 404, Sakado 3-2-1, Takatsu-ku, Kawasaki, Kanagawa 213-0012, Japan.
[3] Medical Engineering Laboratory, Research Center for Medical Science, Jikei University School of Medicine, 3-25-8, Nishi-shinbashi, Minato-ku, Tokyo 105-8461, Japan.
[4] To whom correspondence should be addressed. (e-mail: yoshie@hoshi.ac.jp)

was reported to be independent of liposomal size, surface charge, and PEG molecular weight (5,7,8).

During the past decade, polymeric micelles, supramolecular assemblies of block copolymers, have demonstrated their utility in drug delivery systems and are currently recognized as promising nanocarriers for enhancing the efficacy of drugs and genes (14–16). Since ABC has a considerable impact on the multiple drug administration, it is necessary to study whether the phenomenon is induced by repeated injections of polymeric micelles. Gadolinium (Gd)-based contrast agents are widely used in magnetic resonance imaging (MRI) to improve the conspicuity of lesions or visualization of blood vessels (17). However, these agents are rapidly cleared from the circulation. To overcome this problem, nanocarriers, such as liposomes and polymeric micelles, are used to encapsulate the agents so as to prolong their circulation and allow them to accumulate in tumors for diagnosis (18–20). If polymeric micelles containing a diagnostic agent cause the ABC phenomenon, then circulation time will be reduced after a second dose and the accuracy of the diagnosis will be affected. Furthermore, polymeric micelles containing MRI agents or drugs administered during diagnosis and treatment will lose some of their drug efficacy because of the accelerated clearance. Hence, it is of great importance to know whether the ABC phenomenon can be induced by polymeric micelles or not. Recently, the accelerated clearance of [^{3}H]-labeled PEGylated liposomes was observed in mice pre-administered with an empty polymeric micelle composed of poly (ethylene glycol)-*b*-poly (β-benzyl L-aspartate) (PEG-PBLA) 50 nm in diameter (16).

In this study, we first investigated whether the ABC effect was caused by repeated injections of a polymeric micelle encapsulating Gd-DOTA (Gd-micelle) and of a PEGylated liposome encapsulating Gd-DTPA (Gd-liposome) as a positive control. Concentrations of Gd ions were measured for this investigation. Furthermore, we examined the effect of a PEG homopolymer on the tissue distribution of Gd-liposomes.

MATERIALS AND METHODS

Materials

Magnevist® (Gd-DTPA) was purchased from Bayer Schering Pharma (Berlin, Germany). 1,2-distearoyl-sn-glycero-3-phosphoethanolamine-n-[methoxy(polyethylene glycol)-2000] (mPEG$_{2000}$-DSPE), hydrogenated soy bean phosphatidylcholine (HSPC), and egg phosphatidylcholine (EPC) were purchased from the NOF Corporation (Tokyo, Japan). Cholesterol and polyethylene glycol 500,000 (PEG$_{500,000}$) were of analytical grade (Wako Pure Chemical, Osaka, Japan). All lipids were used without further purification. All other reagents were of analytical grade.

Animals

Four-week-old female ddY mice were purchased from Sankyo Lab Service Corp. (Tokyo, Japan). All care and handling of animals were performed with the approval of the Animal and Ethics Review Committee of Hoshi University and of Principles of Laboratory Animal Care (NIH #publication 85-23, revised in 1985).

Preparation of the Gd-micelle

Synthesis of a chelate moiety-binding block copolymer was performed as reported in our previous paper (19). Briefly, a poly(ethylene glycol)-*b*-poly(L-lysine) block copolymer (PEG-P(Lys)) was prepared through acid hydrolysis of a poly(ethylene glycol)-*b*-poly[ε-(benzyloxycarbonyl)-L-lysine] (PEG-P(Lys(Z)) block copolymer (Fig. 1). We synthesized PEG-P(Lys(Z) with polymerization of a Lys(Z) *N*-carboxy anhydride monomer from PEG-NH$_2$ (molecular weight of PEG-NH$_2$ = 5,200). 1,4,7,10-Tetraazacyclododecane-1,4,7,10-tetraacetic acid mono (*N*-hydroxysuccinimide ester) was fully conjugated to lysine residues of PEG-P(Lys).

The composition of PEG-P(Lys-DOTA) was determined by means of ^{1}H-NMR spectroscopy in D_2O under alkali conditions (pH>10). $GdCl_3 \cdot 6H_2O$ was added to PEG-P(Lys-DOTA) at pH 6.0 to 6.5 for 3 hr at 50°C. Gd content was determined using inductively coupled plasma (ICP) (SPS7800, SII Nano Technology Inc., Tokyo, Japan). We obtained the block copolymer as PEG-P(Lys-DOTA-Gd) (Gd content = 7.7 wt%, the number average of Gd is 8.2). The block copolymer formed a polymeric micelle spontaneously in an aqueous solution (Gd-micelle). The size and zeta-potential of the Gd-micelle diluted with saline for three independent preparations was 84.5±6.0 nm and −1.70±0.80 mV, respectively, at 25°C as determined by dynamic light scattering (ELS-Z2, Otsuka Electronics Co., Ltd., Osaka, Japan).

Preparation of the Empty Liposome and Gd-liposome

First, an empty liposome, which induced the ABC phenomenon, was prepared by the lipid film hydration method as described previously (21). Briefly, a mixture of HSPC, cholesterol, and mPEG$_{2000}$-DSPE in a molar ratio of 1.85:1.0:0.15 was dissolved in chloroform. The solution was

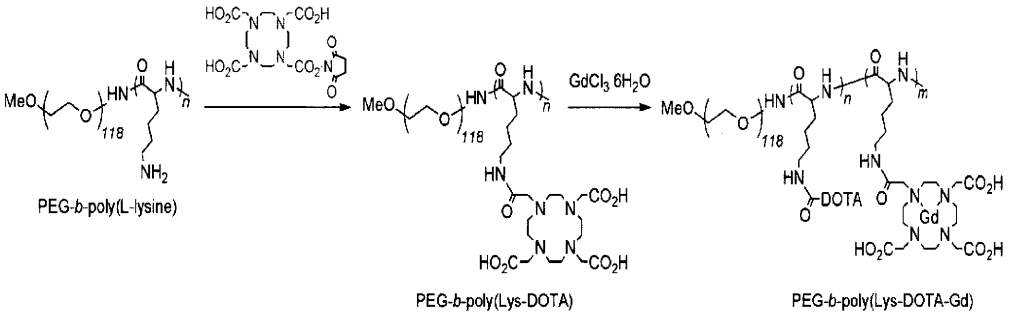

Fig. 1. Synthesis of PEG-P(Lys-DOTA-Gd).

evaporated dry to form the lipid film. Then, the liposome was produced by hydration of the lipid film with saline, followed by size reduction with sonication. The size and zeta-potential of the liposome diluted with saline were 178.5 nm and −22.1 mV, respectively.

Two kinds of Gd-liposomes were prepared because Gd-DTPA content was dependent on the preparation methods. One kind of Gd-liposome was prepared by an ethanol injection method (GdL-E). In brief, a mixture of EPC, cholesterol, and $mPEG_{2000}$-DSPE in a molar ratio of 2.15:0.88:0.15 was dissolved in ethanol and then hydrated with Gd-DTPA at 50°C. The resulting liposomes were sonicated for 10 min, then subjected to exhaustive dialysis against phosphate-buffered saline (PBS, 137 mM NaCl, 8.10 mM Na_2HPO_4, 2.68 mM KCl, 1.47 mM KH_2PO_4, pH 7.4) with a dialysis membrane having a 2,000 molecular-weight cutoff for 24 hr. The size and zeta-potential of the liposome were 150.1±18.8 nm and −0.94±6.78 mV, respectively, for three independent preparations. As a control of GdL-E, an empty liposome not including Gd-DTPA (empty GdL-E) was prepared by the same method as the Gd-liposome (GdL-E), except that saline was used to hydrate the ethanol solution of lipid. The particle size of empty GdL-E was 139.5 nm. Another kind of Gd-liposome was prepared by reverse phase evaporation (GdL-R) to encapsulate a larger amount of Gd-DTPA. The lipid was the same as GdL-E described above and dissolved in 4 mL of chloroform and 2 mL of diethyl ether. Gd-DTPA was added to the lipid solution. The mixture was sonicated to form an emulsion, which was evaporated to produce the liposome. Finally, the resulting liposome was sized at 60°C on an extruder (Avanti Polar Lipids, Inc., AL, USA) with three passes through a 0.4 μm Nuclepore membrane (Waterman, Maidstone, UK) and five passes through a 0.2 μm Nuclepore membrane, followed by exhaustive dialysis as described above. The particle size and zeta-potential of the liposome were 140.9± 13.5 nm and −2.52±5.18 mV, respectively, for three independent preparations. The phospholipid concentration of the liposome including HSPC or EPC was measured with the Phospholipids C-test Wako (Wako Pure Chemical Industries, Ltd.). GdL-E contained 2.26 μmol Gd per 10 μmol lipids, and GdL-R contained 2.29 μmol Gd per 5 μmol lipids.

Release Studies of Gd-micelle and Gd-liposomes

The release of Gd–DTPA from Gd–liposome (GdL–E or GdL–R) and Gd from Gd–micelle was evaluated by dialysis method using a Spectrapor 6 tubing with molecular weight cut-off of 1,000 Da (Spectrum Laboratories Inc., Tokyo, Japan). Briefly, the sample of Gd-micelle containing 1.2 mM Gd and Gd-liposomes of GdL-E containing 0.96 mM Gd-DTPA or GdL-R containing 0.96 mM Gd-DTPA (1 mL) were dialyzed against PBS (pH 7.4, 200 mL) at 37°C. At the indicated time points (10 min, 1, 3, 6, 24 h), 1 mL aliquots of the medium were withdrawn, and the same volume of fresh medium was added. The Gd concentration was analyzed by ICP. The accumulative release of Gd or Gd-DTPA released from the Gd-micelle or Gd-liposome, respectively was expressed as a percentage of the released Gd or Gd-DTPA and plotted as a function of time.

Pharmacokinetics and Tissue Distribution of the Gd-micelle and Gd-liposome

For pharmacokinetics study, the mice were intravenously injected with the Gd-micelle at a dose of 33 μmol Gd/kg (67.3 mg polymer/kg) or the Gd-liposomes including GdL-E at a dose of 6.75 μmol Gd/kg and 10 μmol lipids/kg and GdL-R at 2.65 μmol Gd/kg and 5 μmol lipids/kg. About 30 to 100 μL of blood were taken from a tail vein with a quantitative capillary at 10 min, 1 h, 3 h, 6 h, and 24 h after the injection. The Gd-micelle or the Gd-liposome was injected into a lower part of a tail vein, and blood sample was taken at a certain time point described above from an upper part of the tail vein at the other side of the injected vein. Therefore, this experiment was free from the sample pollution problem. The blood samples were added to saline and centrifuged at 3,000 rpm for 15 min, and the supernatant was used to measure Gd content by ICP. The elimination half-life ($T_{1/2}$) was calculated based on a single compartment model. For the tissue distribution of Gd-micelles and Gd-liposomes study, the second dose of Gd-micelles or Gd-liposomes was injected intravenously through the tail vein at a certain time interval after the first injection. Samples of blood were taken from the hepatic portal vein 6 h after the second injection, and tissues of liver, spleen, and kidney were removed at the same time. The plasma and blood volume were calculated as 0.0488 mL/g body weight for plasma and 0.0778 mL/g body weight for blood, respectively (19).

Measurement of Gd Content

For the quantitative determination of Gd content, blood samples were centrifuged at 3,000 rpm for 15 min, and then plasma was taken out and diluted with 0.1% HNO_3 for ICP. Tissue samples of the liver, spleen, and kidney were digested with a mixture of 98% H_2SO_4 and 62% HNO_3 (1:2, *v:v*) and then subjected to ICP.

Statistical Analysis

The statistical analysis was performed with the Dunnett's multiple comparison test. The level of significance was set at $p<0.05$ or $p<0.01$.

RESULTS

Release Behavior of Gd-micelle and Gd-liposomes

Gd or Gd-DTPA release behavior from Gd-micelle or Gd-liposomes was studied by the dialysis method. As shown in Fig. 2, only 0.2% of Gd leaked from the Gd-micelle at 37°C in PBS (pH 7.4) for 24 h. On the other hand, 4.8% of entrapped Gd-DTPA leaked from the Gd-liposome prepared by reverse phase evaporation method (GdL-R) and 22.4% for 24 h from the Gd-liposome prepared by ethanol injection method (GdL-E). Hence, it is obvious that Gd-micelle has hardly release behavior of Gd, and GdL-R showed much slower release than GdL-E. The results indicated that the leakage of Gd or Gd-DTPA from nanocarriers was greatly affected by the preparation methods.

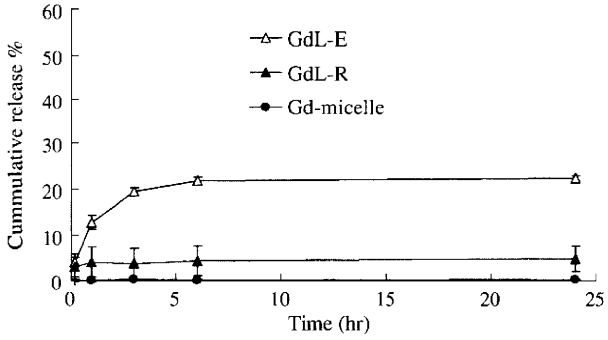

Fig. 2. Release profiles of Gd from Gd-micelle or Gd-DTPA from Gd-liposomes prepared by ethanol injection method (GdL-E) and reverse phase evaporation method (GdL-R) in PBS (pH 7.4) at 37°C. Data represent mean±S.D. (n=3).

Pharmacokinetics of the Gd-micelle and Gd-liposome

As shown in Fig. 3, at 10 min after the intravenous injection, 33.3% of the injected dose was found in blood for the Gd-micelle, and 40.0% and 50.3% for the Gd-liposome of GdL-E and GdL-R, respectively. At a dose of 33 μmol Gd/kg, the $T_{1/2}$ of the Gd-micelle was 10.2±3.9 h. Besides, the $T_{1/2}$ of GdL-E at a dose of 6.75 μmol Gd/kg and GdL-R at a dose of 2.65 μmol Gd/kg were 5.9±0.5 h and 6.0±1.0 h, respectively. In a previous study, we showed that Gd-DTPA was very rapidly cleared from the bloodstream with a minute's order half-life (19). Therefore, the detected Gd in blood is considered to be Gd-DTPA encapsulated in the liposome in a quantitative manner for measurements 6 h post intravenous injection. On the other hand, the main purpose of this study is the ABC phenomenon of a polymeric micelle MRI contrast agent, and PEGylated liposome is used as a positive control for the ABC phenomenon. Therefore, detection of liposome with Gd measurements is appropriate for the present purpose.

Effect of the First Dose on the Distribution of the Gd-micelle

The effects of the first dose on the distribution of the Gd-micelle injected a second time were evaluated. When the second dose of Gd-micelle was fixed at 33 μmol/kg, there was no significant difference of percent injected doses in plasma, kidney, and spleen between various first doses of the Gd-micelle from 0 to 100 μmol/kg (Fig. 4A). A dose of 100 μmol Gd/kg is the clinical dose of Gd-DTPA (17). Interestingly, the distribution of Gd-micelles in plasma, kidney, spleen and liver with the first injection of the empty liposome was similar to that with the first injection of saline. For the liver, the percent injected dose after a first dose of 33 μmol/kg and 100 μmol/kg was significantly higher than in the control saline group, possibly due to the incomplete elimination of the first dose of the Gd-micelle in liver at day 7 because of high doses of polymeric micelles (67.3 mg ~ 203.9 mg polymer/kg). The dose of 2 μmol Gd/kg of the Gd-micelle was the minimum at which Gd was detectable by means of ICP 6 h after injection. As shown in Fig. 4B, when the second dose of the Gd-micelle was decreased to 5 μmol/kg and 2 μmol/kg, the distribution was similar to that of 33 μmol/kg (Fig. 4A). Hence, the results showed that the tissue distribution of the Gd-micelle at the second dose of 33, 5, or 2 μmol/kg was not affected significantly except in liver by pre-administration of the Gd-micelle or the empty liposome. Although Gd in the first dose may interfere with the Gd accumulation in liver following the second dose injection, Gd-micelle as the first dose for micelle-forming properties are

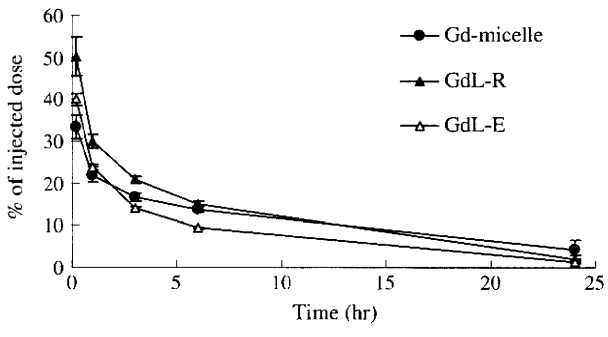

Fig. 3. Plasma elimination profiles of Gd following a single intravenous injection of Gd-micelle at a dose of 33 μmol Gd/kg and Gd-liposome including Gd-liposome prepared by ethanol injection method (GdL-E) at a dose of 6.75 μmol Gd/kg and Gd-liposome prepared by reverse phase evaporation method (GdL-R) at a dose of 2.65 μmol Gd/kg. Data represent mean±S.D. (n=3–4).

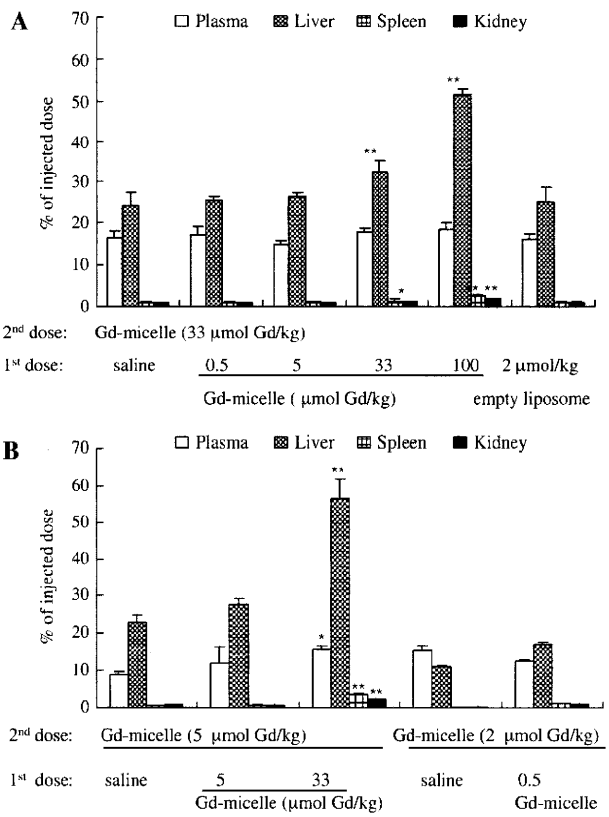

Fig. 4. Effect of the first dose on the tissue distribution of Gd-micelle. The second dose of Gd-micelle with 33 μmol/kg (**A**) or 5 μmol/kg or 2 μmol/kg (**B**) was intravenously injected at day 7 after the first injection of 0.5, 5, 33, 100 μmol/kg of Gd-micelle or the empty liposome at a dose of 2 μmol lipid/kg. Tissues including blood, liver, spleen, and kidney were taken out 6 h after the second injection of Gd-micelle. Data represent mean±S.D. (n=3, 6). P values apply to differences between the saline group and Gd-micelle or liposome treated group. $^{*}p<0.05$, $^{**}p<0.01$.

Gd-content-dependent, and Gd-free polymeric micelle is different from the Gd-containing micelle in size and micelle forming characteristics.

Effect of Time Interval Between the Two Injections on the Distribution of the Gd-micelle

Since it was reported that the ABC effect was maximized when the interval between the two injections of liposome was 10 days in mice (7,12), we changed the time interval for the injection of Gd-micelle at a dose of 33 μmol/kg from 3 days to 10 days. No significant difference in plasma Gd levels (15 ~ 18% dose) was observed between the control group and the groups with different time intervals 6 h after the second injection (Fig. 5). The control group was given the Gd-micelle at 33 μmol/kg after a first injection of saline. The Gd% of injected dose in the liver was much higher at day 3 after the second injection than that on other days, probably due to the incomplete elimination of the first dose of the Gd-micelle.

Effect of the First Dose on the Distribution of the Gd-liposome

Since a lower dose of lipid in the first injection results in a more significant ABC, the effects of dose were investigated. The first dose of the Gd-micelle (5 μmol Gd/kg), empty GdL-E (2 μmol lipids/kg), or GdL-E (2 μmol lipids/kg corresponding to 0.45 μmol Gd/kg) was given with a second dose of GdL-E at 10 μmol lipids/kg corresponding to 2.26 μmol Gd/kg. As shown in Fig. 6, the first injection of the Gd-micelle resulted in a similar percentage of the injected dose of the Gd-liposome in plasma, liver, spleen, and kidney in comparison with the saline group. On the other hand, after the second injection of GdL-E, the Gd concentrations in plasma and kidney were too low to be detected, with the first injection of the empty GdL-E and the GdL-E. At that time, the %dose in the liver significantly increased, but that in spleen significantly decreased as compared to saline ($p<0.05$).

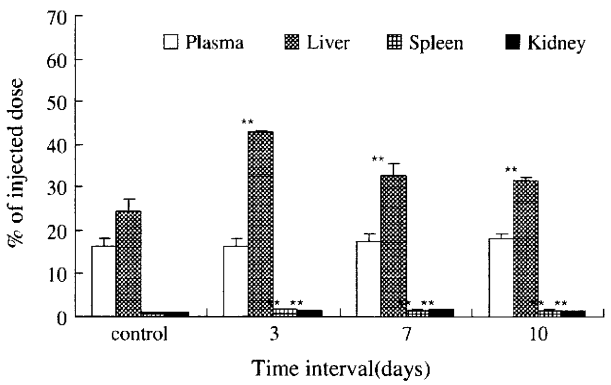

Fig. 5. Effect of the time intervals on the tissue distribution of Gd-micelle. The second dose of Gd-micelle at 33 μmol/kg was intravenously injected at day 3, day 7, or day 10 after the first injection of the same micelle at 33 μmol/kg. The control group was referred to the second dose of Gd-micelle at a dose of 33 μmol/kg with the first injection of saline. Tissues including blood, liver, spleen, and kidney were taken out at 6 h after the second injection of Gd-micelle. Data represent mean±S.D. ($n=3$). *P* values apply to differences between the control group and treated group. $*p<0.05$, $**p<0.01$.

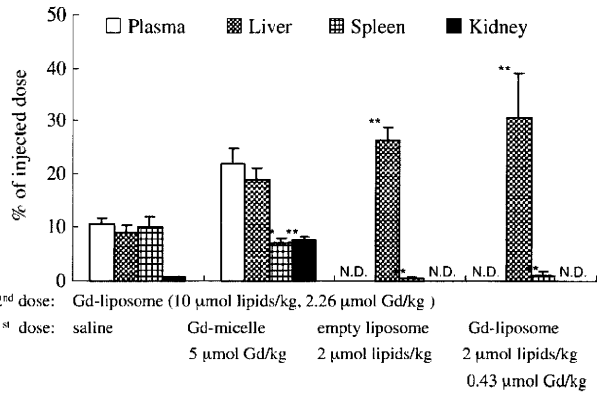

Fig. 6. Effect of the first dose on the tissue distribution of Gd-liposome (GdL-E). The second dose of GdL-E with 10 μmol lipids/kg and 2.26 μmol Gd/kg was intravenously injected at day 7 after the first injection of Gd-micelle (5 μmol Gd/kg), empty GdL-E (2 μmol lipids/kg), and GdL-E (2 μmol lipids/kg and 0.43 μmol Gd/kg). Tissues of blood, liver, spleen, and kidney were removed 6 h after the second injection of GdL-E liposome. Data represent mean±S.D. ($n=3$). *P* values apply to differences between the saline group and Gd-micelle or liposome treated group. $*p<0.05$, $**p<0.01$. N.D. The Gd concentration was too low to be detected by ICP.

Therefore, the data herein show that the accelerated clearance of Gd-liposome at 10 μmol lipids/kg corresponding to 2.26 μmol Gd/kg was induced by both the Gd-liposome and empty liposome, but not by the Gd-micelle. This finding indicates that Gd ions at the first dose of 0.45 μmol/kg did not affect the induction of ABC caused by liposomes.

Effect of PEG on the Distribution of Gd-liposomes

Next, the effect of injecting a PEG homopolymer and PEG_{2000}-DSPE on the distribution of Gd-liposomes was examined. Since the encapsulation efficiency of Gd was low with the ethanol injection method, we prepared another Gd-liposome by the reverse phase evaporation method (GdL-R). The tissue distribution of GdL-R at 6 h after injection at a dose of 5 μmol lipids/kg was not significantly influenced by the pre-administration of 50 mg/kg PEG $_{500,000}$, 0.2 mg/kg PEG $_{500,000}$, or 0.3 mg/kg PEG_{2000}-DSPE 7 days before (Fig. 7). The dose of 0.2 mg/kg PEG $_{500,000}$ and 0.3 mg/kg PEG_{2000}-DSPE with the concentration of 0.04 mg/ml is similar to that of the 5 mol% PEGylated liposome (0.3 mg/kg PEG_{2000}-DSPE), which could produce the ABC phenomenon (Fig. 6). Hence, the first injection of $PEG_{500,000}$ saline or PEG_{2000}-DSPE saline failed to cause the ABC phenomenon after the second administration of Gd-liposome. Hence, only injections of PEG macromolecules did not induce the ABC effect.

DISCUSSION

In the present study, the influence of dose on the tissue distribution of Gd-micelles after repeated administrations was investigated. Many studies have found that a lower dose of lipid in liposomes or nanoparticles results in a greater ABC effect (6–8,12), and the magnitude of the ABC phenomenon reached a maximum when the time interval between two

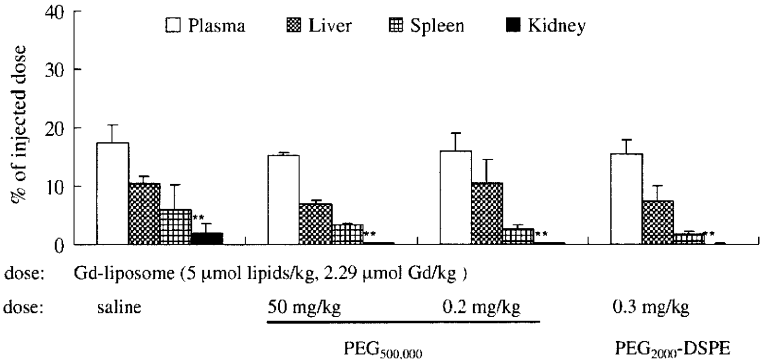

Fig. 7. Effect of $PEG_{500,000}$ and PEG_{2000}-DSPE on the tissue distribution of Gd-liposome (GdL-R). The second dose of Gd-liposome with 5 μmol lipids/kg and 2.29 μmol Gd/kg was intravenously injected at day 7 after the first injection of $PEG_{500,000}$ saline at a dose of 50 mg/kg or 0.2 mg/kg, and PEG_{2000}-DSPE saline at 0.3 mg/kg. The control group of GdL-R was injected at a dose of 10 μmol lipids/kg with the first injection of saline. Tissues of blood, liver, spleen, and kidney were removed at 6 h after the second injection of GdL-R. Data represent mean±S.D. (n=3–5). P values apply to differences between the saline group and $PEG_{500,000}$ or PEG_{2000}-DSPE treated group. $^{*}p<0.05$, $^{**}p<0.01$.

injections was 5–7 days in rats (5) and 10 days in mice (7,12). Hence, we investigated the distribution of the Gd-micelle at various doses and an interval of 3, 7, or 10 days between injections. We found that repeated injections of the Gd-micelle, even with the second dose reduced to 2 μmol Gd/kg (corresponding to 4 mg polymer/kg) and at different time intervals at a dose of 33 μmol Gd/kg (corresponding to 67.3 mg polymer/kg), did not result in an accelerated clearance. ABC of the second injection of the Gd-liposome was induced by the first injection of both the Gd-liposome and the empty PEGylated liposome, but not by the first injection of the Gd-micelle (Fig. 6), Gd-DTPA encapsulated in liposomes would not affect the ABC phenomenon. Therefore, our observation that the ABC phenomenon did not occur with the Gd-micelle is important as it means that injections of the Gd-micelle will not change the biodistribution of a second administration of diagnostic or therapeutic agents.

For Gd-micelle, Gd was chelated to the micelle and thus existed in the form of micelle as shown in Fig. 1, which was consistent with the release results in Fig. 2 that Gd did not leak from the Gd-micelle in PBS (pH 7.4). Gd concentration in plasma, therefore, will reflect the pharmacokinetic behavior of the Gd-micelle. For Gd-liposomes, although the Gd concentration in plasma contained both the leaked Gd-DTPA from the Gd-liposome and the encapsulated Gd-DTPA in the Gd-liposome, the leaked-free Gd-DTPA is reported to be very rapidly cleared from the bloodstream with a minute's order half-life (19), and thus the detected Gd in blood is considered to be only the Gd-DTPA encapsulated in the liposome 6 h after intravenous injection in this study. Compared to GdL-R, the leakage of Gd-DTPA from GdL-E was faster, resulting in the lower Gd concentration (the encapsulated Gd) of GdL-E in blood in Fig. 3. Most importantly, the purpose of this study is to investigate if the distribution for the second dose of the Gd-liposomes or Gd-micelle was affected after pre-administered with the first dose or not. Therefore, the leakage of Gd-DTPA from the Gd-liposomes will not influence this study. In addition, many studies demonstrated that ABC phenomenon for empty liposome was observed determined by [H^3]-labelled or ^{99m}Tc-labelled method (5–9).

It is believed that macrophages in the RES play an important role in ABC, and liposomes were mainly located in Kupffer cells after a second injection (5,8).When hepatosplenic macrophages were depleted, no enhanced clearance of liposomes was observed (6). The induction of ABC with liposomes could be attributable to a 150 kDa serum factor (5), anti-PEG IgM (9,11,12,22,23), anti-PEG antibody (10), or anti-PEG IgG antibody (24).

Whereas the mechanism of the immune response on repeated injections of liposomes has not been fully elucidated yet, the enhanced clearance effect can still be divided into two phases: the induction phase following the first injection and the effectuation phase following the second injection (6). According to this theory, there are two very important factors: one is the biological material (e.g. antibody) produced in the induction phase, the other is the recognition of the antibody by the second dose. For the effectuation phase, it was reported that the ABC phenomenon was induced by the second dose of a PEGylated liposome, but not of a liposome lacking a PEG-coating (23). This indicates that PEG is essential for the nanocarrier to recognize the antibody in the effectuation phase. In this study, the ABC phenomenon was not observed after repeated injections of the Gd-micelle at different doses and time intervals. This ABC failure of Gd-micelle may be caused by the failure for the production of biological material in the induction phase (data not shown) or/and for the recognization by the antibody in the effectuation phase. Even if the first injection was of empty liposome, the second injection of the Gd-micelle did not produce the ABC phenomenon either. This suggests that the antibody produced by the empty liposome in the induction phase is not recognized by the PEG moiety of the Gd-micelle. Therefore, not only PEG, but also other factors such as structure and hydrophobic character affect recognition.

For the induction phase, the ABC phenomenon was not observed when the amount of PEGylated lipid of liposomes in the first injection was more than 10 mol% (7,8). We have previously reported the accelerated clearance of [^{3}H]-labeled PEGylated liposomes in mice pre-administered empty PEG-PBLA polymeric micelles (16). Furthermore, repeated

injections of PEG-PLA nanoparticles also produced the ABC phenomenon (12). Hence, the structure and component of nanocarriers has a considerable impact on the induction phase of ABC. From a structural perspective, the Gd-micelle formed through ionic interactions; therefore, it does not have any hydrophobic part (Fig. 1). In contrast, the PEG-PBLA micelle is composed of both a hydrophilic part, PEG, and a hydrophobic part, PBLA. Similarly, PEGylated liposomes possess a hydrophilic PEG chain and a hydrophobic bilayer membrane. The immunogenicity of an antigen can be affected by factors such as the physical and chemical properties of the antigen, its dose, and so on (25). The reasons why the Gd-micelle evaded the ABC phenomenon have not yet been elucidated at the present stage. The absence of a hydrophobic part may be a key for this elucidation because the other ABC-phenomenon-positive PEG-based carrier systems possess hydrophobic part in a hydrophobic inner core for polymeric micelles and in a lipid bilayer for PEG-liposomes. We are currently investigating the ABC phenomenon induced by other kinds of polymeric micelles and nanoparticles. It is hoped that these experiments will provide more evidence for the mechanism of the ABC phenomenon.

CONCLUSIONS

The Gd-micelle did not induce ABC following its pre-administration at various doses and time intervals. In contrast, the Gd-liposome induced the phenomenon when it or an empty PEGylated liposome, but not the $PEG_{500,000}$ macromolecule or PEG_{2000}-DSPE, was pre-administered. ABC-phenomenon-positive PEG-based carrier systems possess a hydrophobic part in a hydrophobic inner core for polymeric micelles and in a lipid bilayer for PEG-liposomes. The absence of a hydrophobic part of Gd-micelle may be a key factor for not producing the ABC phenomenon.

ACKNOWLEDGMENTS

This study was supported by the Ministry of Health, Labour, and Welfare of Japan. We also acknowledge the support from the Program for Promoting the Establishment of Strategic Research Centers, Special Coordination Funds for Promoting Science and Technology and the Ministry of Education, Culture, Sports, Science and Technology of Japan.

REFERENCES

1. Allen TM, Hansen C, Martin F, Redemann C, Yau-Young A. Liposomes containing synthetic lipid derivatives of poly(ethylene glycol) show prolonged circulation half-lives *in vivo*. Biochim Biophys Acta. 1991;1066:29–36.
2. Woodle MC, Lasic DD. Sterically stabilized liposomes. Biochim Biophys Acta. 1992;1113:171–99.
3. Lasic DD, Martin FJ, Gabizon A, Huang SK, Papahadjopoulos D. Sterically stabilized liposomes: a hypothesis on the molecular origin of the extended circulation times. Biochim Biophys Acta. 1991;1070:187–92.
4. Torchilin VP, Omelyanenko VG, Papisov MI, Bogdanov AA Jr, Trubetskoy VS, Herron JN, *et al.* Poly(ethylene glycol) on the liposome surface: on the mechanism of polymer-coated liposome longevity. Biochim Biophys Acta. 1994;1195:11–20.
5. Dams ET, Laverman P, Oyen WJ, Storm G, Scherphof GL, van Der Meer JW, *et al.* Accelerated blood clearance and altered biodistribution of repeated injections of sterically stabilized liposomes. J Pharmacol Exp Ther. 2000;292:1071–9.
6. Laverman P, Carstens MG, Boerman OC, Dams ET, Oyen WJ, van Rooijen N, *et al.* Factors affecting the accelerated blood clearance of polyethylene glycol-liposomes upon repeated injection. J Pharmacol Exp Ther. 2001;298:607–12.
7. Ishida T, Ichikawa T, Ichihara M, Sadzuka Y, Kiwada H. Effect of the physicochemical properties of initially injected liposomes on the clearance of subsequently injected PEGylated liposomes in mice. J Control Release. 2004;95:403–12.
8. Ishida T, Harada M, Wang XY, Ichihara M, Irimura K, Kiwada H. Accelerated blood clearance of PEGylated liposomes following preceding liposome injection: effects of lipid dose and PEG surface-density and chain length of the first-dose liposomes. J Control Release. 2005;105:305–17.
9. Ishida T, Kiwada H. Accelerated blood clearance (ABC) phenomenon upon repeated injection of PEGylated liposomes. Int J Pharm. 2008;354:56–62.
10. Judge A, McClintock K, Phelps JR, Maclachlan I. Hypersensitivity and loss of disease site targeting caused by antibody responses to PEGylated liposomes. Mol Ther. 2006;13:328–37.
11. Semple SC, Harasym TO, Clow KA, Ansell SM, Klimuk SK, Hope MJ. Immunogenicity and rapid blood clearance of liposomes containing polyethylene glycol–lipid conjugates and nucleic acid. J Pharmacol Exp Ther. 2005;312:1020–6.
12. Lu W, Wan J, She ZJ, Jiang XG. Brain delivery property and accelerated blood clearance of cationic albumin conjugated pegylated nanoparticle. J Control Release. 2007;118:38–53.
13. Gabizon A, Isacson R, Rosengarten O, Tzemach D, Shmeeda H, Sapir R. An open-label study to evaluate dose and cycle dependence of the pharmacokinetics of pegylated liposomal doxorubicin. Cancer Chemother Pharmacol. 2008;61:695–702.
14. Kakizawa Y, Kataoka K. Block copolymer micelles for delivery of gene and related compounds. Adv Drug Deliv Rev. 2002;54:203–22.
15. Yokoyama M, Okano T, Sakurai Y, Ekimoto H, Shibazaki C, Kataoka K. Toxicity and antitumor activity against solid tumors of micelle-forming polymeric anticancer drug and its extremely long circulation in blood. Cancer Res. 1991;51:3229–36.
16. Koide H, Asai T, Hatanaka K, Urakami T, Ishii T, Kenjo E, *et al.* Particle size-dependent triggering of accelerated blood clearance phenomenon. Int J Pharm. 2008;362:197–200.
17. Lin SP, Brown JJ. MR contrast agents: physical and pharmacologic basics. J Magn Reson Imaging. 2007;25:884–99.
18. Mulder WJ, Strijkers GJ, van Tilborg GA, Griffioen AW, Nicolay K. Lipid-based nanoparticles for contrast-enhanced MRI and molecular imaging. NMR Biomed. 2006;19:142–64.
19. Shiraishi K, Kawano K, Minowa T, Maitani Y, Yokoyama M. Preparation and in vivo imaging of PEG-poly(L-lysine)-based polymeric micelle MRI contrast agents. J Control Release. 2009;136:14–20.
20. Nakamura E, Makino K, Okano T, Yamamoto T, Yokoyama M. A polymeric micelle MRI contrast agent with changeable relaxivity. J Control Release. 2006;114:325–33.
21. Wang XY, Ishida T, Ichihara M, Kiwada H. Influence of the physicochemical properties of liposomes on the accelerated blood clearance phenomenon in rats. J Control Release. 2005;104:91–102.
22. Ishida T, Ichihara M, Wang XY, Yamamoto K, Kimura J, Majima E, *et al.* Injection of PEGylated liposomes in rats elicits PEG-specific IgM, which is responsible for rapid elimination of a second dose of PEGylated liposomes. J Control Release. 2006;112:15–25.
23. Wang XY, Ishida T, Kiwada H. Anti-PEG IgM elicited by injection of liposomes is involved in the enhanced blood clearance of a subsequent dose of PEGylated liposomes. J Control Release. 2007;119:236–44.
24. Sroda K, Rydlewski J, Langner M, Kozubek A, Grzybek M, Sikorski AF. Repeated injections of PEG-PE liposomes generate anti-PEG antibodies. Cell Mol Biol Lett. 2005;10:37–47.
25. Abbas AK, Lichtman AH, Pober JS. Cellular and molecular immunology. Philadelphia: Saunder; 1991.